Received 6 November 2021; accepted 28 November 2021. Date of publication 8 December 2021; date of current version 22 December 2021.

Digital Object Identifier 10.1109/OJCOMS.2021.3133543

IMPRESS: Indoor Mobility Prediction Framework for Pre-Emptive Indoor-Outdoor Handover for mmWave Networks

AYSENUR TURKMEN (Graduate Student Member, IEEE), SHUJA ANSARI (Senior Member, IEEE), PAULO VALENTE KLAINE, LEI ZHANG (Senior Member, IEEE), AND MUHAMMAD ALI IMRAN (Senior Member, IEEE)

James Watt School of Engineering, University of Glasgow, Glasgow G12 8QQ, U.K.

CORRESPONDING AUTHOR: A. TURKMEN (e-mail: a.turkmen.1@research.gla.ac.uk)

This work was supported in part by EPSRC Resource Orchestration for Diverse Radio Systems (REORDER) Project under Grant EP/S02476X/1. The work of Aysenur Turkmen was supported by the Republic of Turkey Ministry of National Education under Grant MoNE-1416/YLSY.

This paper has been presented in part at the IEEE Wireless Communications and Networking Conference (WCNC) 2021 [1].

ABSTRACT Millimeter-wave (mmWave) communication, the main success behind the fifth generation of mobile communication networks, will increase the ultra-dense small cell deployment under its limited coverage characteristics. Therefore, providing a seamless connection to its users, to whom transitioning between indoor and outdoor in a heterogeneous network environment particularly is a significant issue that needs to be addressed. In this paper, we present a two-fold contribution with a comprehensive study on mm-wave handovers. A user-based indoor mobility prediction via Markov chain with an initial transition matrix is proposed in the first step. Based on this acquired knowledge of the user's movement pattern in the indoor environment, we present a pre-emptive handover algorithm in the second step. This algorithm aims to keep the QoS high for indoor users when transitioning between indoor and outdoor in a heterogeneous network environment. The proposed algorithm shows a reduction in the handover signalling cost by more than 50%, outperforming conventional handover algorithms.

INDEX TERMS mmWave 5G, Markov Chain, online learning, user trajectory, indoor mobility, pre-emptive handover, femtocells, heterogeneous network indoor-to-outdoor handover.

I. INTRODUCTION

The FIFTH Generation (5G) of the mobile network is a game-changer technology since it promises to meet the significant data demand of the 21st century. The first phase of 5G's practical implementations have already begun at a global scale, and its second phase (mmWave 5G) plans are moving forward [2]. Cities around the world, such as the U.K. and China for instance, they have already deployed 5G in their major cities, promising low latency in high data rate communications [3].

The mmWave frequency band ranges in the spectrum from 3 to 300 GHz [4] and is the main factor of the 5G's achievement for enabling high data rates with minimum latency. Moreover, the mmWave bandwidth provides almost ten times the capacity of its predecessor cellular networks [5], [6]. Although mmWave bandwidth is an excellent feature for the next generation of wireless communications, they come with a severe loss of penetration problem. The coverage footprint of mmWaves are relatively smaller than the previous generations, as the wavelength gets smaller while frequency increases because of the physical nature of radio communications.

Ultra dense small network (UDN) is one the practical solution to this issue, in which mmWave frequency driven small cells (SCs) are densely deployed over an area, in order to increase the network coverage [4]. However, careful management and regulations are needed in UDN; otherwise the number of handovers would increase wherein SCs are densely deployed. In the presence of frequent handover occurrences, two essential parameters of a network: Quality of Experience (QoE) and the Quality of Service (QoS) of users are affected negatively. Furthermore, studies conducted by 3GPP show that the HO failure rate in a heterogeneous macro-pico network is up to 60%, that is twice higher compared to a macro-only network [7]. Additionally, frequency sharing, energy efficiency, resource management, user association, interference management, and the economics of this ultra-dense network are some of the challenging areas that have yet to be addressed [4]. The high number of plug-and-play SCs placement especially in the residential areas may notably degenerate the QoS because of the severe inter-cell interference (ICI) [8]. Network slicing in the mm-wave could be one of the feasible solutions to the aforementioned challenges by establishing the framework of air-interface heterogeneous signal orchestration and efficient resource allocation. To ensure the best mmWave coverage for indoor users, mmWave driven femto base station, FBS, need to be deployed inside the building. Therefore indoor users would reach the high data rate communications provided by mmWave frequencies. However, mmWave's great exposure to the penetration loss creates the coverage holes between indoor and outdoor environment served by mmWave SCs. Hence, the user will receive an abrupt drop on Received Signal Strength (RSS) when moving out from indoor FBS coverage to outdoor SC coverage.

As a promising approach to ensure seamless connectivity, predictive mobility management can predict future locations of user equipment (UE) as well as the HO requests of UE, hence the next network BSs could be prepared for incoming HO requests. It is essential to consider the environment and network for predictive mobility management, as it needs some input that can be useful for machine learning algorithms, for example. The importance of mobility prediction in wireless communications has prompted numerous studies to investigate the subject. In [9], the authors used Markov chains to predict the user movement and highlight the impact of the transition probability matrix, which was built based on their assumptions. As part of their work in [10], the authors used the users' mobility history to input a transition probability matrix, which was used to uncover the most frequently visited base stations. To reduce the HO delay in 4G X2 HO, [11] proposes a machine learning model for managing the mobility the part of the HO process to improve prediction of future HOs. In order to solve the path dependency problems arising from classical Markov chains, which occur when users access the same cell repeatedly, the authors introduced a 3D transition matrix. A mobility prediction model using Markov Chains has been developed in [12] for 4G data plane networks. They introduced a trajectory dependency parameter, therefore, their proposed model's reaction to less frequent and random movements could be controlled by a trajectories dependency parameter.

Despite the fact that indoor users generate nearly 80% of the mobile traffic [13], however, the majority of the studies mainly focused on the mobility prediction in outdoor environment. Moreover, when the Covid-19 pandemic situations

TABLE 1. Literature comparison.

Ref.	Technology		Environment		Management	
	LTE	5G	Indoor	Outdoor	Handover	Mobility
[9]	✓					✓
[10]	✓					✓
[11]	✓			✓	✓	
[12]	✓			✓	✓	✓
[16]	✓		✓		✓	
[17]	✓		✓		✓	
[18]	✓		✓		✓	
This work		✓	✓	✓	✓	✓

are considered, i.e., restrictions such as local/national lockdowns, homeschooling and paradigm shift to working from home, are led to people spending more time indoors, which further increases the data demand for indoor users. For instance, Vodafone reported that the Internet usage by their contractors is already seen up to 50% in some European countries as the impact of Covid-19, and the demand is expected to be even higher depending on rules that governments implement, such as working from home [14].

The handover management of users from indoors to outdoors has not received the necessary attention, even though most of the traffic demand is created from indoor users [15]. The authors of [16] used Kernel methods to reduce the ping-pong handover occurrences when an indoor UE moves close to areas where the outdoor macro BS's signal strength increases, such as the corner of a window or a door. Yet, the study only focuses on when the user is indoors. In [17], handover delay optimization for femtocell users are done by predicting the next cell. In [18], a dual handover triggering scheme is proposed for indoor users, where some additional event parameters are introduced. Even though the mentioned studies approach a common problem of reducing the ping-pong handovers and the handovers when the UE moves from indoor to outdoor (I_2O) [17], [18]; the studies are conducted in a 4G-LTE environment whose coverage size of macro BSs can be of several kilometres. Table 1 gives a brief insight of the difference between our work and the surveyed studies above.

According to real-world measurements of 28 GHz and 73 GHz in [5], the coverage size of mmWaves will have a small footprint of around 100–200 meters, which brings us to the necessity of an intelligent and seamless I_2O handover management scheme. Considering the fact that Because SCs will be deployed both indoors and outdoors, with a much higher density, it is crucial that they are deployed efficiently, and are supported by mobility predictions. Even more so, high penetration losses would create mmWave-driven indoor environments isolated from the outdoors [15]. As such, due to this isolation and sharp change of RSS, when a UE passes through a door; call drops would be inevitable.

These studies are the basis of our motivation to present the following twofold contributions in this paper.

- First, we introduce an Indoor Mobility Prediction model for mmWave CommunicationS using Markov ChainS

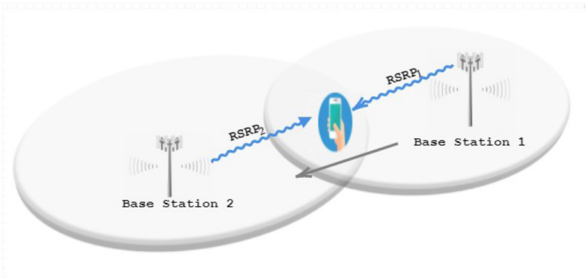

FIGURE 1. Handover illustration.

(IMPRESS), in which Markov chains are utilized in favor of preemptive handovers for a user-centric indoor mobility prediction.

- Second, by relying on IMPRESS, we present a preemptive indoor to outdoor (I_2O) handover algorithm in order to reduce the latency within the indoor and outdoor multi-tier network, while a user transitions among them.

The remainder of this paper is organized as follows. Section II delivers the background information on HO in general and, specifically its management in New Radio (NR). Section III-A, introduces the IMPRESS algorithm, while Section III-B presents the preemptive I_2O handover algorithm. The results are presented in Section IV. Finally, Section V concludes this paper and its contributions.

II. HANDOVER MANAGEMENT OVERVIEW

A. HANDOVER IN MOBILE COMMUNICATION SYSTEMS

Handover or handoff is a procedure of maintaining steady connection of a UE to the network when it moves out from the serving cell's coverage to another cell's coverage. The procedure is done by changing the current cell's channel into a new channel whenever the UE moves into a new cell [19].

Fig. 1 demonstrates a simple handover scenario where the UE that is attached to BS_1 has an on going call while moving towards to the coverage area of BS_2. The UE continuously monitors the signal strength of the two base stations (BS_1 and BS_2). If the measured signal strength of the BS_2 goes higher than BS_1 in the overlapping area, and the BS_2 can provide the required resources that the UE needs a handover process will be performed to connect the UE to the BS_2; avoiding the disconnection of the ongoing call.

The call dropping probability (CDP) and the call blocking probability (CBP) are two essential parameters that give a clear indicator for the QoS of a network in the context of mobility. CDP happens when the handover process is rejected, and the connection is dropped due to the required resources of the connection not being supported by the new BS. Alternatively, the probability of new connection access being denied by the target BS due to current traffic congestion is called CBP. The use of bandwidth (channel) or the efficient utilisation of frequency bands within a network is another fundamental parameter of QoS. For more information about CDP and CBP readers should go to [20], [21].

In general, there are three phases in a handover procedure: measurement, handover decision and handover execution. The outcome of the first stage, the measurement report, is input along for the handover algorithms of the second stage. In the last stage, handover is executed by assigning a UE to the new BS, and hence the old connection is terminated. In the handover decision phase, if measurements are done by the UE and the network conducts the handover decision, it is called Mobile Assisted Handover (MAHO). Whereas if the decision is made by the network using the measurements collected from the UEs at several BSs, it is called Network Controlled Handover (NCHO). Lastly, Mobile Controlled Handover (MCHO) is where each UE thoroughly assists in the handover process [19].

In addition, a HO can also be categorized as a soft or hard handover. In the hard handover, which is mostly employed in Time Division Multiple Access (TDMA) and Frequency Division Multiple Access (FDMA), the connection with the existing BS is ended before a new connection is made with the target BS. The soft handover, mostly utilized in Code Division Multiple Access (CDMA), preserved the existing connection while making a new connection with a target BS.

1) HANDOVER REQUIREMENTS

Handovers in the wireless network might have a negative effect on both the QoS and the capacity of the network if the aspects mentioned below are not taken into account.

- Handover latency should be kept as low as possible.
- The total number of handovers should be kept minimum in case of knowing the particular trajectory of a UE.
- Additional signals should be lowered during the handover process.
- Handover impact on QoS should be minimized, such as lowering CDPs and CBPs, as well as the traffic between the neighboring cells.

There are also some factors need to be considered from the designers aspect to achieve the desired features of handovers. Some of them are.

- *Cellular structure* has an important effect on handover occurrence, depending on the size of a cell. For instance, if the cell size decreases, handover becomes more frequent for a given mobile user scenario. Macro-cell, micro-cell, pico-cell, and femto-cell are wireless network types, ordered by their cell size [22].
- *Mobility*, referring to the direction and speed of the user, also has an impact on the handovers. For example, the handover requirements might differ for a user that moves fast, in a car, or a train etc., and a user with a normal speed. Therefore, the handover algorithms should address the different types of requirements based on the user's needs.
- The decrease in *QoS*; such as bandwidth, BER or packet loss, might trigger the handover in order to find another BS that can provide a better QoS.

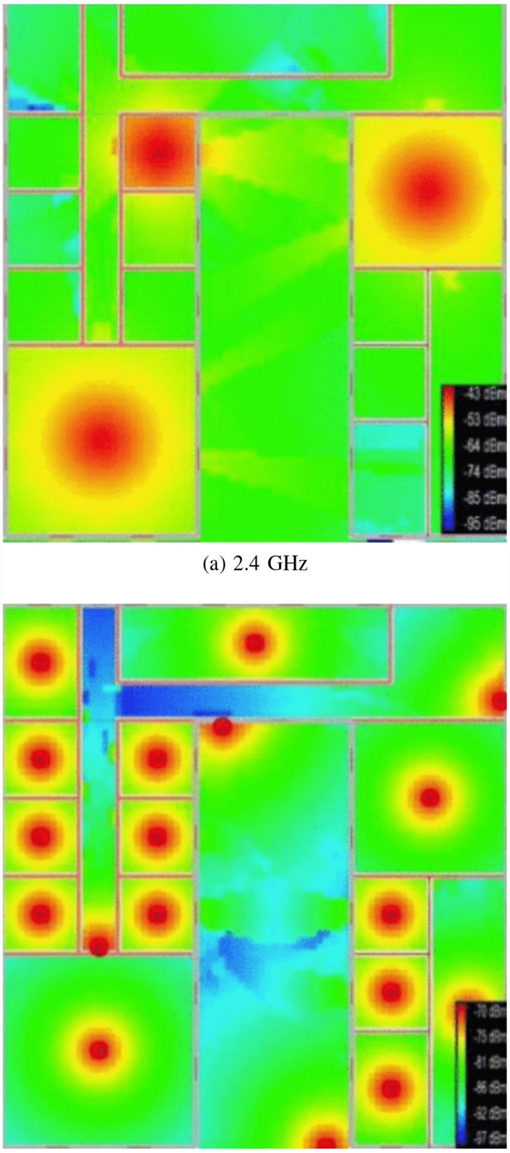

(a) 2.4 GHz

(b) 60 GHz

FIGURE 2. Coverage of the same building with 2.4 GHz and 60 GHz [23].

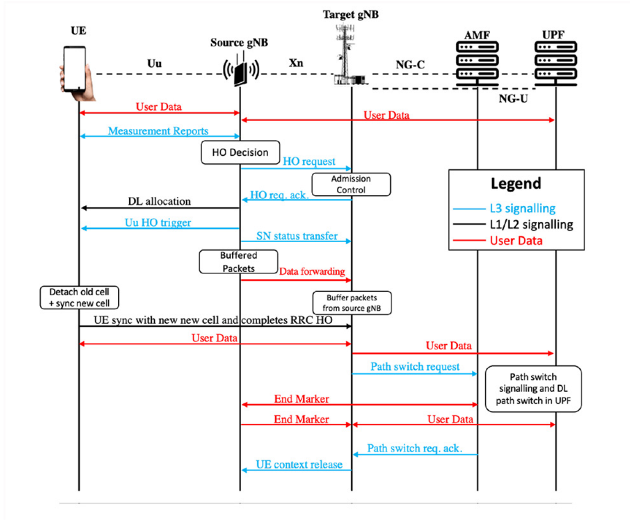

FIGURE 3. Handover in 5G NR.

B. HANDOVER IN MMWAVE COMMUNICATION SYSTEMS

Handover management in mmWave communication systems is an important subject, which needs to be addressed properly. As shown in Fig. 2, to cover the same building, the mmWave antenna needs to be installed in nearly all rooms, since it has a smaller coverage footprint than conventional networks [23].

Users mobility in this small size of coverage area would trigger several handovers [24], which may cause the total number of handovers to increase during a call (ping pong effect). As seen from Fig. 2 a), in previous networks, such as GSM, UMTS, 802.11 WLAN, LTE, there is adequate time for the initiation and completion of a handover successfully, as overlapping areas between cells are quite large. However, with greater frequencies in mmWave systems, the coverage size decreases rapidly. Thus, the overlapping area gets smaller. Mainly in an indoor environment, overlapping areas typically occur around open spaces such as doors and windows. For instance, once a UE leaves a room through a door, the UE can make a sharp turn, turning left or right. In this case, a handover may not be completed successfully if not detected early enough since the overlapping area might be too small to allow the UE enough time to complete a handover. This phenomenon is called the corner effect, and it needs to be taken into consideration, especially in higher frequencies. Reference [23] addresses the time taken for a handover in 60 GHz networks in an indoor environment, where they assumed a user with a 2 m/s movement speed in a 10 by 10 meters room size.

Fig. 3 demonstrates the basic handover procedure in NR, the latest radio access technology developed by 3GPP for the 5G mobile network [25]. There are two types of NG Radio Access Network nodes connected to the 5G core network that are gNB and ng-eNB. A gNB supports NR control-plane and user-plane protocols to the NR devices and, an ng-eNB uses the LTE control-plane and user-plane protocols to serve the LTE devices [26]. The procedure begins by checking if a UE needs a handover.

1) By sending measurement reports to the source gNB, next generation Node B in 5G.
2) handover decision is made in the serving gNB, using RRM (Radio Resource Management) information and the measurement report.
3) The handover request message, including the required data for preparing the HO at the target BS side, is sent from the connected gNB to the target gNB.
4) Admission Control procedure will be performed in this step, if the target gNB can grant the resources.
5) The target gNB sends a handover request acknowledgement message to the serving gNB, and the

forwarding of data can be initiated once the serving gNB receives it.
6) UE receives the handover command from the serving gNB.
7) The Sequence Number (SN) message is sent from serving gNB to the target gNB to keep track of the ordering of the packets.
8) The UE disconnects from the serving gNB and synchronizes to the target gNB.
9) The target gNB informs AMF that UE has changed the cell via the Path Switch Request message.
10) NR core shifts the DL data path towards the target side.
11) The path switch request acknowledgement is sent by the AMF to the target gNB.
12) The serving gNB receives successful handover information from the target gNB, and activates the release of resources via UE context release message.

The radio resources related to the UE are released eventually by the serving gNB [27].

C. CELL RANGE EXTENSION

The RSRP plays an essential role in determining a handover (connected mode) and conventional cell selection (idle mode) since the decisions are based on it [28]. In a heterogeneous network environment, macro cells have higher transmit power up to 16 dB than SCs [29]; therefore users inherently choose macro cells over SCs, when assessing the downlink reception. However, this situation would make SC implementation redundant, and the resources of SCs would not be fully exploited, which may cause overloading on the macro cells. In order to cope with the problem, a cell range extension, CRE, is presented in [30], where a bias value is added to the received signal of SC. Thus, SC coverage is increased virtually, and more UEs can make a connection to the pico cells, resulting in offloading on macro BSs [31], as described by

$$\left(w_p^{pilot}\right)_{dB} + (\Delta_{bias})_{dB} > \left(w_m^{pilot}\right)_{dB}, \tag{1}$$

where $(w_p^{pilot})_{dB}$, $(w_m^{pilot})_{dB}$, and $(\Delta_{bias})_{dB}$, are the decibel value of pilot signal from pico and macro BSs, and bias value respectively, [32].

III. METHODOLOGY

As this study provides a twofold contribution, we first present the methodology used for Indoor Mobility PREdiction for mmWave CommunicationS using Markov ChainS - IMPRESS- along with the proposed solution for the defined problem in Section III-A. Secondly, the proposed preemptive Indoor-to-Outdoor (I_2O) mmWave handover algorithm is presented and its results are evaluated.

A. INDOOR MOBILITY PREDICTION AND PROPOSED SOLUTION FOR IMPRESS FRAMEWORK

Indoor user mobility is one of the critical factors of today's system-level simulations; as stated in [13], indoor users generate almost80% of mobile traffic. Based on the studies in [33]–[36], the user's mobility is stated to have some pattern and is not entirely spontaneous. On the contrary, it is target-oriented [35], as humans do not walk around erratically but rather aim for a particular goal, for instance, leaving home to go to a train station or heading to the kitchen from the living room. Using human decision-making process in [36], [37] modelled user mobility as a non-random manner. The authors in [37] evaluated this decision making process as a product of two factors; external and internal, in which the former is represented by environment stimulus and group behaviour, whereas individual characteristics indicate the latter.

As evidenced by the studies highlighted above, we hypothesise that a user's movement shows more regularities in an indoor environment than in an outdoor environment since degrees of freedom are lower in the indoor scenario than in an outdoor scenario. Considering these regularities, we have designated a particular area in our indoor model, called a cloakroom, where users usually go to pick up their shoes, coats, keys, umbrellas, etc., before going out, and vice versa. Based on this hypothesis, we aim to capture this regularity pattern of the user in the environment given in Fig. 4 by using Markov Chains. To evaluate the indoor user's probabilities of transitioning in each room of the building, we model the indoor environment by segmenting each indoor region (IR) into the Markov Chain states. In [1], we presented the user's mobility by using two techniques for initializing the Transition Matrix (TM) of Markov Chain; *Online Learning TM* and *Q-Learning of TM*. Due to the complexity of the latter one, where the system might need some data for training purposes [1], we conducted our study using an online learning TM method for determining the mobility trajectory of a user. The following gives a better sight of the used technique in the IMPRESS algorithm.

- *Markov Chain in Mobility Prediction:* Markov chains play a key role in stochastic processes, and they are mostly applied for predictions in a randomly changing systems. In the Markov chain, the occurrence of the next state is not determined by the previous state, but by the current state, therefore it is associated as memory-less [9]. A set of states builds up a Markov chain, and in our scenario we assigned these states to the indoor regions depicted in the Fig. 4. Fig. 5 illustrates the Markov chain states $S = \{IR_1, IR_2, \ldots, IR_n\}$ in this study, where $\mathbb{I} = \{1, 2, \ldots, n\}$ is the states' indices and transitions $t_{i,j}$ symbolize the probability of user's movement between the states. The probability of transition to the next state in Markov chain is mathematically modelled as:

$$\begin{aligned}&\mathbb{P}(S_{n+1} = s_{n+1} | S_n = s_n, \ldots, S_1 = s_1)\\&\quad = \mathbb{P}(S_{n+1} = s_{n+1} | S_n = s_n).\end{aligned} \tag{2}$$

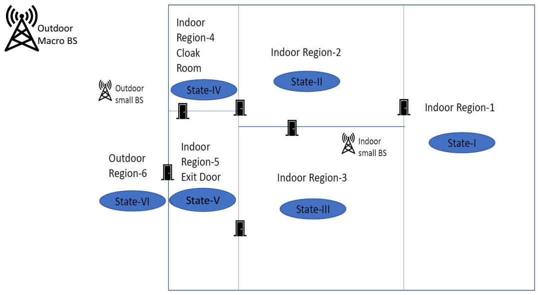

FIGURE 4. System Model showing Indoor Regions as Markov Chain states.

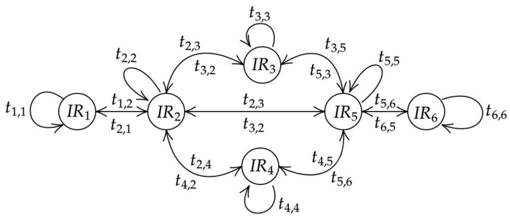

FIGURE 5. Discrete-time Markov Chain with 6 finite state spaces (i.e., IRs).

According to our proposed scheme, the states of the Markov chain are defined as indoor regions (IRs) within an indoor environment, as opposed to the studies in Section I, where the states are defined as base stations. To determine which state the UE is in, the RSS (Received Signal Strength) method is used, which is a simple and widely used technique [38]. The probability distribution is obtained from:

$$\mathbf{p}_k = \mathbf{p}_0 \mathbf{T}^k, \tag{3}$$

$$\mathbf{T} = \begin{bmatrix} t_{1,1} & t_{1,2} & \cdots & t_{1,n} \\ t_{2,1} & t_{2,2} & \cdots & t_{2,n} \\ \vdots & \vdots & \vdots & \vdots \\ t_{n,1} & t_{n,2} & \cdots & t_{n,n} \end{bmatrix}, \tag{4}$$

in which $\mathbf{p}_k$ represents the k$^{\text{th}}$ transition probability vector, $\mathbf{p}_0$ is the initial distribution vector and $\mathbf{T}$ is the transition probability matrix.

- *Updating Transition Matrix With Online Learning:* As it is highlighted through out the paper that movements of the users are target oriented, we propose to use the online learning for initialising the transition matrix of the Markov chain. Our assumption is that HO is initiated by the UE, the updating procedure of transition matrix $\mathbf{T}$ is based on the user's movement in the indoor environment. We assign a higher probability to the most common routes taken by the user than to the other routes. Before initializing the transition matrix, the below setting are made, which are: 1) The transition matrix is set to right stochastic matrix, $\sum_{j=1}^{n} t_{i,j} = 1, \forall i \in \mathbb{I}$, and, 2) The transition matrix is a hallow matrix, as any state transition itself is not allowed: $t_{i,i} = 0, \forall i \in \mathbb{I}$. We consider the assumption that the UE initiates the HO transition, and the updating process of transition matrix $\mathbf{T}$ is done by using the tracked position of the user. Based on the user's movement in the indoor environment illustrated in Fig. 4, the high probability value is assigned to the trajectory UE follows most. Following the method in [12], a trajectory dependency variable R_d, $0 \leq R_d \leq 1$, is applied to adjust the model's learning rate and response to random or less frequent motions. The High (small) rate of R_d signifies that updating the transition matrix has high (low) trust, which gives great (small) control on the user's trajectory on the updated $\mathbf{T}$. For instance, a situation like $R_d = 1$ implies that the prediction will be biased to the most recent trajectory, whereas $\mathbf{T}$ will not be updated in the extreme situation of $R_d = 0$ as the prediction is not related to the user's trajectory [12]. For a more detailed explanation of the update procedure of $/textbf[T]$, consider the following example: $IR_1 \longrightarrow IR_2 \longrightarrow IR_3$. The UE updates the probabilities of outbound movements from IR_1 to all neighboring IRs after each movement between two regions, e.g., from IR_1 to IR_2, in an iterative game scheme with many stages. Amounts controlled by R_d increase the probability of outbound UE movement from IR_1 to IR_2, while attempts to direct UE movement from IR_1 towards all playing IRs are decreased. This is expressed as:

$$t_{1,2} = t_{1,2} + \sum_{j} t_{1,j} R_d, j \in \mathbb{N}_{IR_1}, \tag{5}$$

$$t_{1,j} = t_{1,j} - \frac{\sum_j t_{1,j} R_d}{\left|\mathbb{N}_{IR_1}\right| - 1}, j \in \mathbb{N}_{IR_1}, \tag{6}$$

where $|\mathbb{N}_{IR_1}|$ is the cardinality of the set of neighboring IRs for IR_1 which are taking part in the game. To satisfy the condition of inclusivity ($0 \leq t_{i,j} \leq 1$), a lower bound of 0 and an upper bound of 1 is set for each entry in $\mathbf{T}$. It then becomes necessary to satisfy the condition of right stochastic matrix. The solution is to add additional stages that approach equilibrium without violating the conditions of transition matrix [12].

B. PREEMPTIVE I_2O HANDOVER FRAMEWORK

The rapid drop in SINR due to the penetration loss, especially when a UE moves from the door of a building, is verified by the field measurements conducted in [18]. However, the mentioned study above is conducted by utilizing LTE frequencies. Since mmWave driven networks are far greater prone to penetration losses than LTE, we present a preemptive I_2O handover scheme for a UE transitioning from indoor to outdoor under a heterogeneous network environment. The proposed scheme aims to perform the HO process beforehand the out-of-synchronization (out-of-sync) happens; to avoid a rapid decline in communication quality.

1) PROPOSED SCHEME TO I_2O HANDOVER

Mobility is the most important parameter for handover management. When its proper configurations are done, it can lower the number of handovers. Thus the handover cost could be reduced. Therefore, in the IMPRESS algorithm, the information about the user's indoor trajectory on the most visited rooms (states) before the user goes out are considered *(MVSBGO)*. In the second contribution of this study, *I_2O handover*, we build a realistic simulation scenario of a multi-tier heterogeneous network, where mmWave driven femto and picocell BSs are deployed in the presence of a macro BS. The UE's trajectory information before going out is obtained in Section III-A, which is in this scenario, the user mostly visits the state-IV (also can be called as cloakroom in here), then follows the state-V and state-VI to go out. After acquiring this information, we designated a particular area in the state-V called *HO spot area*, which is 0.5 meters away from the exit door of the building. When the user comes to the *HO spot area* while being in the active state, our pre-emptive *I_2O handover algorithm* checks the trajectory history of the user to obtain the information of whether this history contains the coordinates of the state-IV or not. If the user's mobility trajectory history contains the coordinate of the state-IV, the *I_2O handover algorithm* initiates the handover signalling, similar to the A3 event in the LTE. But with the only difference is that in the LTE A3 event, handover is triggered, and the measurement report is sent from the UE when the received RSRP of the serving cell goes below the RSRP of the neighbouring cell over a pre-defined period named time-to-trigger (TTT), which is defined as in [18]:

$$RSRP_n - RSRP_s > A3offset_s - CIO_{n,s}, \tag{7}$$

where RSRP_n and RSRP_s the RSRP of the neighbouring and the serving base stations, respectively. $\mathrm{A3offset}_s$ is the offset of the serving cell, and $\mathrm{CIO}_{n,s}$ is the cell individual offset between the neighbouring and serving cells. However, in our case, the RSRP of the serving cell -femtocell here-only goes below the threshold or the RSRP of neighbouring cells when the UE goes out of the exit door and leaves the building. Instead of starting the handover signalling after the UE leaves the building, we propose initiating the handover signalling before the UE leaves the building. More precisely, the HO process will be initiated at the *HO spot area*, as it is illustrated in Fig. 6 to maintain the continuity of the user's ongoing active session.

Otherwise, because of the high penetration losses for mmWaves, the user would face an abrupt drop in the received power, resulting in a reduction of the QoE. Eventually, a call drop would happen. The RSRP plays an essential role in a conventional cell selection (idle mode) and handover (connected mode) as the decisions depend on it [28]. Therefore, to enable the proposed scheme, an additional offset value (CREO) is added to the RSRP of the closest outdoor small BS to extend its cell range. Thus, the handover process should be initiated preemptively to prevent out-of synchronization (out-of-sync) when the UE leaves the building. The detailed pseudo code of the proposed handover algorithm for the *I_2O handover algorithm* is explained in Algorithm 1.

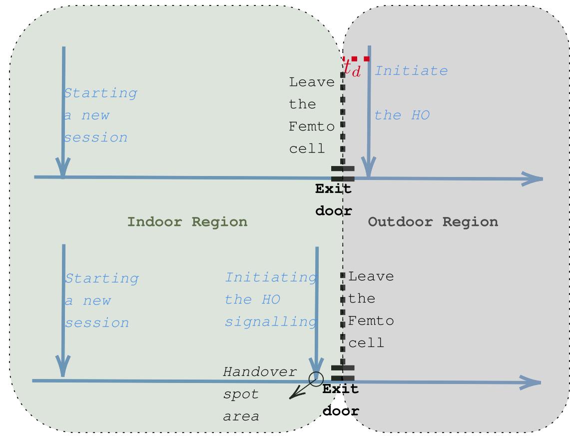

FIGURE 6. The timing diagram of proposed I_2O handover.

Algorithm 1 Algorithm for Preemptive I_2O Handover

Input: SINR, UE location, UE trajectory history, HO spot area, CREO.
Output: SNRoutBS

Initialization:
Mobility Management : Initialization of UE transition matrix to find probabilities of visited states in indoor
Output: probability of most visited state before going out-*MVSBGO-*
HO preemption:
if $UE_{currentlocation} = HO_{spotarea}$ **then**
  check the UE trajectory history
  if $UE_{trajectoryhistory} = MVSBGO$ **then**
    $SNRoutBS = SNRoutBS + offset$
    $reward = 1$ for doing so, otherwise $reward = 0$
  end if
end if

2) PROPAGATION MODEL FOR I_2O HANDOVER

The surrounding environment and the maximum radius of the cell, which have a substantial impact on the received signal, are two of the most critical characteristics that affect wireless coverage. The received signal parameters are principally affected by three factors: multipath (small-scale) fading, shadow (large-scale) fading, and, path loss propagation. A zero-mean Gaussian random variable with a logarithmic variance is used to simulate the features of fading. Thus, a radio propagation model based on the well-known log-distance path loss model in [39] has been adapted and implemented as:

$$PL_{in} = P0_{in} + 10\gamma_{in}\log_{10}(d/d0_{in}) + \delta + \rho_{drywall} + \varrho, \tag{8}$$

$$PL_{out} = P0_{out} + 10\gamma_{out}\log_{10}(d/d0_{out}) + \delta + \rho_{concrete} + \varrho, \tag{9}$$

TABLE 2. Simulations and deployment parameters.

Simulations Parameters	Parameter Value
Carrier frequency for FBS and SBS (GHz) [41]	28
Carrier frequency for MBS (MHz) [42]	3
Bandwidth of FBS and SBS (MHz) [43]	100
Bandwidth of MBS (MHz) [44]	20
Transmit power of FBS (dBm) [45]	30
Transmit power of SBS (dBm) [46]	35
Transmit power of MBS (dBm) [45]	46
Concrete ρ at 28 GHz [15]	34.1
Concrete ρ at 3 GHz [15]	17.7
Drywall ρ at 28 GHz [15]	6.8
γ_{in} [47]	1.6
γ_{out} [47]	3
Number of outdoor base stations	2
Number of indoor base stations (femtocells)	1
Antenna type (indoor/outdoor) [15]	Half-wave dipole

where PL is the total path loss in decibel (dB) at a distance d in meters, and $P0$ is the free-space path loss at the reference distance $d0$. γ is the path loss exponent, δ is the Gaussian random variable with zero mean, $\rho_{drywall}$ and $\rho_{concrete}$ are the penetration loss exponents for each specific material. Lastly, ϱ is the shadow fading of the channel.

As it can be seen in (8) and (9), the path loss is calculated separately for both mmWave indoor and outdoor small BSs, and macro BS. These calculations are done by denoting the parameters into the specified frequency values for indoor and outdoor for the equations mentioned above. The specifications for the simulation parameters are stated in Table 2. The SINR of the system is calculated as:

$$SINR = \frac{P_r}{\sigma^2 + I}, \tag{10}$$

where Pr is the received power in watt, derived by subtracting the pathloss from the transmit power of relevant BS. σ^2 is the noise power density and I is the interference of the neighboring cells.

IV. SIMULATION RESULTS

A. IMPRESS SIMULATION RESULTS

As shown in Fig. 4, the simulation environment has six Markov states. The states between state I and state V stand for the indoor environment, and state VI represents the outdoor environment. The system calculates the possibilities for a 100-day series with six transitions every day. Each day, a single user is subject to four different mobility scenarios.

- 0% of random data: UE follows the pre-defined route.
- 10%, 20% and 50% random data: UE follows the random routes depending on the randomness weight of the data.

In order to reward the system, reward 0 is assigned to each step that UE has taken between the states, aside from state V (HO spot area) and state VI (outside). For these states (V and VI), rewards 25 and 100 are assigned, respectively.

The result of prediction accuracy of *IMPRESS* for various R_d values is presented in Fig. 7.

As the transition matrix T is initialized with equiprobable values over all possible states, it can be seen that for

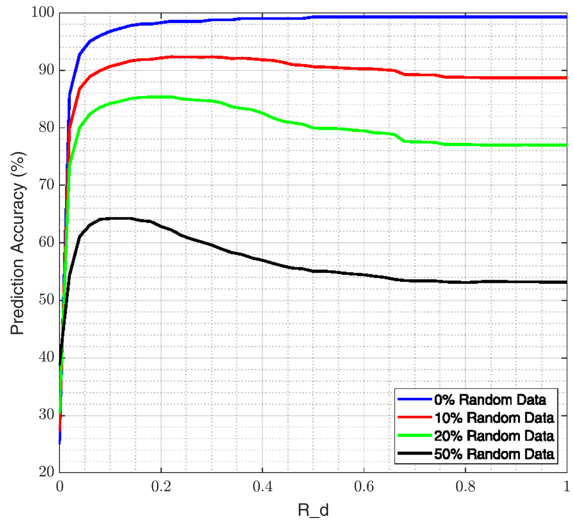

FIGURE 7. Accuracy for different values of R_d for initial transmission matrix T.

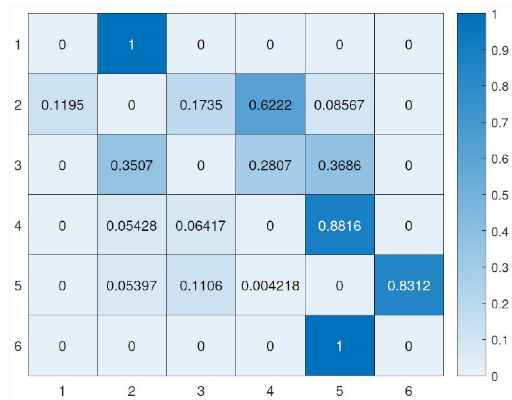

FIGURE 8. Transition matrix T for $R_d = 0.2$.

low values of R_d, the prediction accuracy is very low, with accuracy ranging from 25% to 40% for the different mobility models when $R_d = 0$. This happens because the Markov chain model does not assume prior user mobility knowledge, resulting in an initial learning time. The algorithm makes wrong predictions more often than correct ones. However, as R_d increases, we can see that the prediction accuracy reaches values of 98 - 99% when no randomness is considered and declines for higher values of R_d for the other mobility models. This occurs because when R_d is higher, the transition matrix updates faster; thus, when randomness is introduced, it is less reliable [12].

Fig. 8 demonstrates the heatmap of initialized transition matrix probabilities at $R_d = 0.2$ with a 50% randomness in user mobility. It clearly shows the high probabilities assigned to each state that the UE is expected to follow, even with the presence of high randomness.

B. PREEMPTIVE I_2O HANDOVER RESULTS

The measured SINR values for the simulation environment with three scenarios are presented in Fig. 9. At first, we

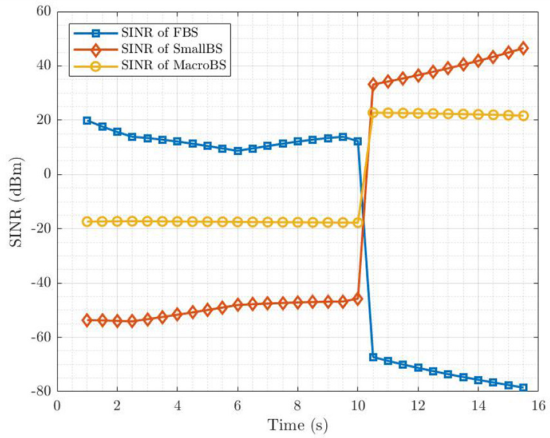

(a) Measured $SINR$ result without any algorithm is applied, Scenario 1.

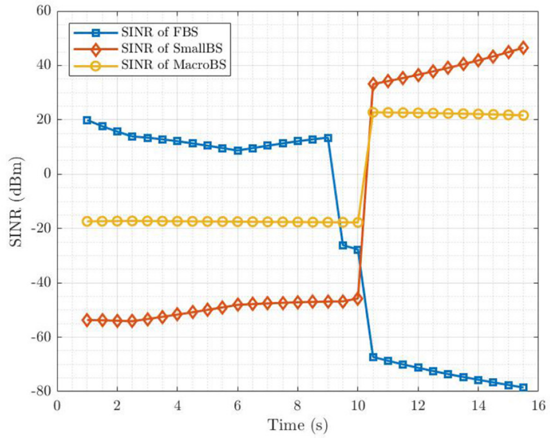

(b) Negative offset value is added to the FBS received power, Scenario 2.

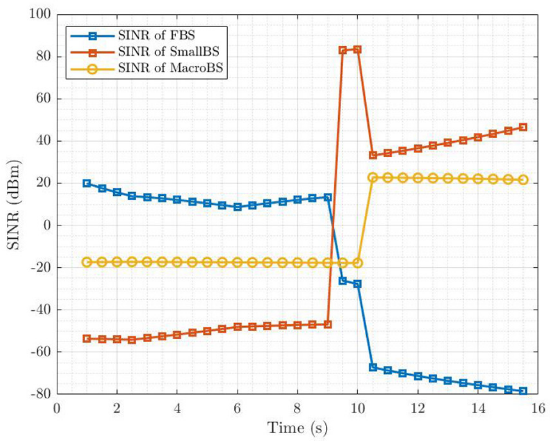

(c) Presented algorithm is applies to the received power of FBS and SC BS, Scenario 3.

FIGURE 9. **Measured SINR values for the simulation environment.**

began our simulations by deploying only small cells at 28 GHz to imitate the UDN environment; however, in real life, these environments are mostly underlaid by the macro BSs. Therefore we improved our simulations by adding macro BS serving at 3GHz, and the interference between these frequencies are shown in Fig. 9. The first scenario in Fig. 9(a) shows the SINR measurements, in which the handover algorithm is not applied. As it is seen, the FBS has the highest SINR value of 20 dBm compared with the other two outdoor BSs having SINR of −20 dBm and −55 dBm. However, when the UE moves to outdoor, there is an abrupt drop on the SINR of the FBS dropping to below −60 dBm, while the SINR of outdoor BSs increases swiftly. This result proves our hypothesis about the need for a proper handover algorithm for indoor users while transitioning to the outdoors. Otherwise, because of these abrupt changes seen in Fig. 9(a), it is inevitable to avoid the connection losses, which will reduce the QoS of the communication network. Fig. 9(b) shows where the negative offset value is added to the FBS' received power when UE is at the handover spot area. In this case, the UE will preemptively connect to the macro BS. However, there will be another handover in a very short time when UE moves outside, as SC BS has a higher SINR than the macro BS. The extra loading on the macro BS and the unnecessary handover occurrence in this scenario shows that this scenario is not feasible. Hence, we propose adding a positive offset value to the closest small BS' SINR value, as shown in Fig. 9(c); this way, the UE can connect pre-emptively to the SC BS before moving outdoor. Therefore, the positive offset is added to the closest small BS's SINR value as we proposed in Algorithm 1 Step 7 ($2 \times SINR_{outdoorBS}$). Thanks to this rapid increase from the offset value shown in Fig. 9(c) the user can accommodate the closest small BS preemptively, avoiding the ping pong between macro and small outdoor BSs. Thus, transitioning between these two BSs becomes seamless while maintaining the QoS, as we aim to reduce the latency[1] by initiating advance preparation of the HO procedure.

C. I_2O HANDOVER SIGNALLING COST

To evaluate the performance of the proposed I_2O handover algorithm, HO signalling cost is employed. The required time for delivering and processing the signalling messages is stated as the transmission cost, and processing cost in [47]. The one-way transfer delay between a pair of nodes is the transmission cost; the delay in processing one message in one node is the processing cost. Despite the lengths of handover messages are varied, we use the assumption made in [47] for simplicity, i.e., transmission cost for different messages among the same pair of nodes are the same regardless of the message size. A similar assumption goes with the processing time, i.e., the processing time is the same for the different messages at the same node. Moreover, we follow [12] by assuming that the mobility management entity (MME) and the serving gateway (S-GW) are located in the same location. Therefore the transmission delay among these nodes is constant and can be neglected.

1. In mmWave driven UDN whose coverage isolated because of the high penetration losses.

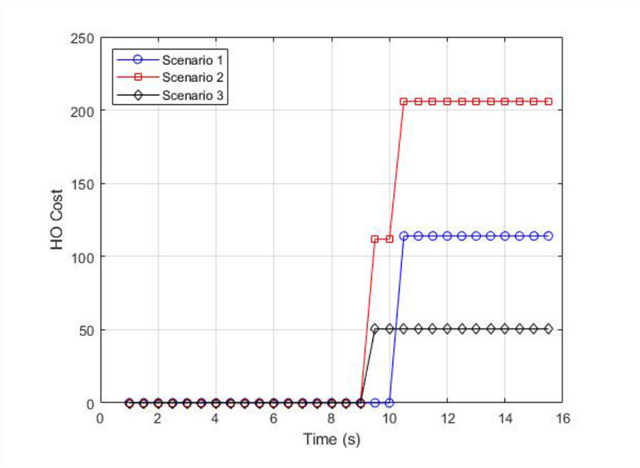

FIGURE 10. HO signalling cost for the proposed scenarios.

The HO signalling cost, C_{HO} provided in Fig. 10 for the three different scenarios discussed in previous sections, is calculated by [48]:

$$C_{HO} = \sum \psi_{i,j} + \sum \gamma_i, \tag{11}$$

where $\psi_{i,j}$ is denoted as the one way transmission cost among nodes i and j, and γ_i is the processing cost in node i. Scenario 1 is the regular case where a traditional handover algorithm is implemented. In scenario 2, the SINR of the FBS is decreased by an offset value to enable the comparison observations between scenario 3. Finally, scenario 3 is where the proposed I_2O algorithm is implemented by adding a positive offset value to the nearest small BS in the outdoor. As it is clearly seen that the proposed algorithm applied in scenario 3 outperforms the other two scenarios by more than 50%, bringing the signalling costs from 115 in scenario 1 to only 50 in scenario 3.

V. CONCLUSION

This paper has a two-fold contribution with a comprehensive study on mmWave handovers. First, a user-based indoor mobility prediction via Markov chain with an initial transition matrix is proposed, acquired from Q-learning algorithms. Results show that the model using an initial transition matrix has slightly higher accuracy, with a price of more complexity, as the system needs prior training based on historical data. Therefore, we propose an online learning method for the transition matrix when no user mobility data is available. Based on this acquired knowledge of the user's mobility in the indoor environment, among other functionalities, preemptive handovers for mmWave communications can be applied to reduce handover latency in the densely deployed SC networks. In the second step, depending on the user's indoor mobility history acquired from the first step, we propose a pre-emptive indoor to outdoor handover algorithm to maintain the high QoS for indoor users transitioning between indoor and outdoor regions in a heterogeneous network environment. The implementation and evaluation of our proposed algorithm show a reduction in the handover signalling costs by more than 50%, outperforming conventional handover algorithms. Since mmWave networks are now being commercially deployed in indoor environments, as future work, the proposed IMPRESS framework and the proposed handover algorithm will be applied to scale up dense femto cell deployments in order to analyze the performance in a more comprehensive and real-life scenario.

REFERENCES

[1] A. Turkmen, S. Ansari, P. V. Klaine, L. Zhang, and M. A. Imran, "Indoor mobility prediction for mmWave communications using Markov Chain," in *Proc. IEEE Wireless Commun. Netw. Conf. (WCNC)*, 2021, pp. 1–5.

[2] I. Shayea, M. Ergen, M. Hadri Azmi, S. A. Çolak, R. Nordin, and Y. I. Daradkeh, "Key challenges, drivers and solutions for mobility management in 5G networks: A survey," *IEEE Access*, vol. 8, pp. 172534–172552, 2020.

[3] BBC News, "China Rolls Out 'One of the World's Largest' 5G Networks." (2019). [Online]. Available: https://www.bbc.co.uk/news/business-50258287. (Accessed: Jun. 24, 2020).

[4] N. Al-Falahy and O. Y. K. Alani, "Millimetre wave frequency band as a candidate spectrum for 5G network architecture: A survey," *Phys. Commun.*, vol. 32, pp. 120–144, feb 2019.

[5] M. R. Akdeniz *et al.*, "Millimeter wave channel modeling and cellular capacity evaluation," *IEEE J. Sel. Areas Commun.*, vol. 32, no. 6, pp. 1164–1179, Jun. 2014.

[6] A. M. Al-Samman *et al.*, "Comparative study of indoor propagation model below and above 6 GHz for 5G wireless networks," *Electronics*, vol. 8, no. 1, p. 44, 2019.

[7] J. G. Andrews, "Seven ways that hetnets are a cellular paradigm shift," *IEEE Commun. Mag.*, vol. 51, no. 3, pp. 136–144, Mar. 2013.

[8] Y. Wang, G. Feng, Y. Sun, S. Qin, and Y.-C. Liang, "Decentralized learning based indoor interference mitigation for 5g-and-beyond systems," *IEEE Trans. Veh. Technol.*, vol. 69, no. 10, pp. 12124–12135, Oct. 2020.

[9] N. Amirrudin, S. H. S. Ariffin, N. N. N. A. Malik, and G. N. Effiyana, "Mobility prediction via markov model in lte femtocell," *Int. J. Comput. Appl.*, vol. 65, no. 18, pp. 40–44, 2013.

[10] N. A. Amirrudin, S. H. S. Ariffin, N. N. N. A. Malik, and N. E. Ghazali, "User's mobility history-based mobility prediction in LTE femtocells network," in *Proc. IEEE Int. RF Microw. Conf. (RFM)*, 2013, pp. 105–110.

[11] M. Ozturk, P. V. Klaine, and M. A. Imran, "3D transition matrix solution for a path dependency problem of markov chains-based prediction in cellular networks," in *Proc. IEEE 86th Veh. Technol. Conf. (VTC-Fall)*, 2017, pp. 1–5.

[12] A. Mohamed, O. Onireti, S. A. Hoseinitabatabaei, M. Imran, A. Imran, and R. Tafazolli, "Mobility prediction for handover management in cellular networks with control/data separation," in *Proc. IEEE Int. Conf. Commun. (ICC)*, 2015, pp. 3939–3944.

[13] E. Perez, K.-J. Friederichs, A. Lobinger, B. Wegmann, and I. Viering, "Erratum to: Utilization of licensed shared access resources in indoor small cells scenarios," in *Cognitive Radio Oriented Wireless Networks*, D. Noguet, K. Moessner, and J. Palicot, Eds. Cham, Switzerland: Springer, 2016, p. E1.

[14] The Guardian, "Vodafone Reports 5% Rise in Internet Use As More People Work From Home," (2020). [Online]. Available: https://www.theguardian.com/business/2020/mar/18/vodafone-rise-data-usage-more-people-work-from-home-coronavirus

[15] M. A. Imran, A. Turkmen, M. Ozturk, J. Nadas, and Q. H. Abbasi, "Seamless indoor/outdoor coverage in 5G," Wiley, May 2020, pp. 1–23. [Online]. Available: https://doi.org/10.1002%2F9781119471509.w5gref227

[16] N. Sinclair, D. Harle, I. A. Glover, and R. C. Atkinson, "A kernel methods approach to reducing handover occurrences within LTE," in *Proc. Eur. Wireless 18th Eur. Wireless Conf.*, 2012, pp. 1–8.

[17] T.-H. Kim and J.-W. Kim, "Handover optimization with user mobility prediction for femtocell-based wireless networks," *Int. J. Eng. Technol. (IJET)*, vol. 5, no. 2, pp. 1829–1837, 2013.

[18] T. Inoue, Y. Watanabe, T. Nobukiyo, and Y. Matsunaga, "Dual handover triggers to improve QoE for indoor and outdoor mobility," in *Proc. IEEE 25th Annu. Int. Symp. Pers. Indoor Mobile Radio Commun. (PIMRC)*, 2014, pp. 1727–1731.

[19] I. Stojmenovic, *Handbook of Wireless Networks and Mobile Computing*. Hoboken, NJ, USA: Wiley, 2002.

[20] L. Yu *et al.*, "Step: A spatio-temporal fine-granular user traffic prediction system for cellular networks," *IEEE Trans. Mobile Comput.*, vol. 20, no. 12, pp. 3453–3466, Dec. 2021.

[21] M. Mamman, "Call admission control algorithm with efficient handoff for both 4G and 5G networks," *Int. J. Wireless Mobile Netw. (IJWMN)* vol. 13, no. 3, p. 8, 2021.

[22] Z. Xiao, H. Liu, V. Havyarimana, T. Li, and D. Wang, "Analytical study on multi-tier 5G heterogeneous small cell networks: Coverage performance and energy efficiency," *Sensors*, vol. 16, no. 11, p. 1854, 2016.

[23] B. V. Quang, R. V. Prasad, and I. Niemegeers, "A survey on handoffs–Lessons for 60 GHz based wireless systems," *IEEE Commun. Surveys Tuts.*, vol. 14, no. 1, pp. 64–86, 1st Quart., 2012.

[24] B. L. Dang, M. G. Larrode, R. V. Prasad, I. Niemegeers, and A. Koonen, "Radio-over-fiber based architecture for seamless wireless indoor communication in the 60GHz band," *Comput. Commun.*, vol. 30, no. 18, pp. 3598–3613, Dec. 2007.

[25] S. Lien, S.-L. Shieh, Y. Huang, B. Su, Y.-L. Hsu, and H. Wei, "5G new radio: Waveform, frame structure, multiple access, and initial access," *IEEE Commun. Mag.*, vol. 55, no. 6, pp. 64–71, Jun. 2017.

[26] E. Dahlman, S. Parkvall, and J. Sköld, "Radio-interface architecture," in *5G NR: The Next Generation Wireless Access Technology*. Amsterdam, The Netherlands: Elsevier, 2018, pp. 73–102.

[27] M. Tayyab, X. Gelabert, and R. Jantti, "A survey on handover management: From LTE to NR," *IEEE Access*, vol. 7, pp. 118907–118930, 2019.

[28] M. Jaber, M. A. Imran, R. Tafazolli, and A. Tukmanov, "An adaptive backhaul-aware cell range extension approach," in *Proc. IEEE Int. Conf. Commun. Workshop (ICCW)*, 2015, pp. 74–79.

[29] M. Jaber, M. Imran, R. Tafazolli, and A. Tukmanov, "An adaptive backhaul-aware cell range extension approach," in *IEEE International Conference on Communication Workshop (ICCW)*, 2015, pp. 74–79, doi: 10.1109/ICCW.2015.7247158.

[30] Q. Europe, "R1–083813: Range expansion for efficient support of heterogeneous networks," 3GPP TSG RAN WG1 Meeting, Tech. Rep., Sept. 20O8.
Ericsson *et al.* "Text proposal for evaluation methodology," 3GPP TSG RAN WG1, Rep. R1-083807, Sep. 2008.

[31] T. Kudo and T. Ohtsuki, "Cell range expansion using distributed Q-learning in heterogeneous networks," in *Proc. IEEE 78th Veh. Technol. Conf. (VTC Fall)*, 2013, pp. 1–5.

[32] D. López-Pérez and X. Chu, "Inter-cell interference coordination for expanded region picocells in heterogeneous networks," in *Proc. 20th Int. Conf. Comput. Commun. Netw. (ICCCN)*, 2011, pp. 1–6.

[33] P. S. Prasad and P. Agrawal, "Mobility prediction for wireless network resource management," in *Proc. 41st Southeastern Symp. Syst. Theory*, 2009, pp. 98–102.

[34] D. M. Rose, T. Jansen, S. Hahn, and T. Kürner, "Impact of realistic indoor mobility modelling in the context of propagation modelling on the user and network experience," in *Proc. 7th Eur. Conf. Antennas Propag. (EuCAP)*, 2013, pp. 3979–3983.

[35] J. Kolodziej *et al.*, "An application of markov jump process model for activity-based indoor mobility prediction in wireless networks," in *Proc. Front. Inf. Technol.*, 2011, pp. 51–56.

[36] B. Tang, C. Jiang, H. He, and Y. Guo, "Probabilistic human mobility model in indoor environment," in *Proc. Int. Joint Conf. Neural Netw. (IJCNN)*, 2016, pp. 1601–1608.

[37] D. Helbing and P. Molnar, "Social force model for pedestrian dynamics," *Phys. Rev. E, Stat. Phys. Plasmas Fluids Relat. Interdiscip. Top.*, vol. 51, no. 5, p. 4282, 1995.

[38] F. Zafari, A. Gkelias, and K. K. Leung, "A survey of indoor localization systems and technologies," *IEEE Commun. Surveys Tuts.*, vol. 21, no. 3, pp. 2568–2599, 3rd Quart., 2019.

[39] A. Goldsmith, *Wireless Communications*. Cambridge, U.K.: Cambridge Univ. Press, 2005.

[40] A. Turkmen *et al.*, "Coverage analysis for indoor-outdoor coexistence for millimetre-wave communication," in *Proc. UK/China Emerg. Technol. (UCET)*, 2019, pp. 1–4.

[41] S. Zhao, Y. Feng, and G. Yu, "D2d communication channel allocation and resource optimization in 5g network based on game theory," *Comput. Commun.*, vol. 169, pp. 26–32, Mar. 2021.

[42] D. Wisely, N. Wang, and R. Tafazolli, "Capacity and costs for 5g networks in dense urban areas," *IET Commun.*, vol. 12, no. 19, pp. 2502–2510, 2018.

[43] C. B. Barneto, L. Anttila, M. Fleischer, and M. Valkama, "Ofdm radar with lte waveform: Processing and performance," in *Proc. IEEE Radio Wireless Symp. (RWS)*, 2019, pp. 1–4.

[44] Y. Sun, G. Feng, S. Qin, Y.-C. Liang, and T.-S. P. Yum, "The smart handoff policy for millimeter wave heterogeneous cellular networks," *IEEE Trans. Mobile Comput.*, vol. 17, no. 6, pp. 1456–1468, Jun. 2018.

[45] Z. Li, C. Wang, and C.-J. Jiang, "User association for load balancing in vehicular networks: An online reinforcement learning approach," *IEEE Trans. Intell. Transp. Syst.*, vol. 18, no. 8, pp. 2217–2228, Aug. 2017.

[46] S. Hussain, "Efficient ray-tracing algorithms for radio wave propagation in urban environments," Ph.D. dissertation, School Electron. Eng., Dublin City Univ., Whitehall, Ireland, 2017.

[47] J. S. M. Ho and I. F. Akyildiz, "Local anchor scheme for reducing signaling costs in personal communications networks," *IEEE/ACM Trans. Netw.*, vol. 4, no. 5, pp. 709–725, Oct. 1996.

[48] L. Wang, Y. Zhang, and Z. Wei, "Mobility management schemes at radio network layer for LTE femtocells," in *Proc. VTC Spring IEEE 69th Veh. Technol. Conf.*, 2009, pp. 1–5.